

Search for weakly decaying Λn and $\Lambda\Lambda$ exotic bound states in central Pb-Pb collisions at $\sqrt{s_{NN}} = 2.76 \text{ TeV}$

(ALICE Collaboration) Adam, J.; ...; Antičić, Tome; ...; Erhardt, Filip; ...; Gotovac, Sven; ...; Mudnić, Eugen; ...; ...

Source / Izvornik: **Physics Letters B, 2016, 752, 267 - 277**

Journal article, Published version

Rad u časopisu, Objavljena verzija rada (izdavačev PDF)

<https://doi.org/10.1016/j.physletb.2015.11.048>

Permanent link / Trajna poveznica: <https://urn.nsk.hr/urn:nbn:hr:217:884291>

Rights / Prava: [Attribution 4.0 International](#)/[Imenovanje 4.0 međunarodna](#)

Download date / Datum preuzimanja: **2024-04-25**



Repository / Repozitorij:

[Repository of the Faculty of Science - University of Zagreb](#)





Search for weakly decaying $\bar{\Lambda}n$ and $\Lambda\Lambda$ exotic bound states in central Pb–Pb collisions at $\sqrt{s_{NN}} = 2.76$ TeV

ALICE Collaboration*



ARTICLE INFO

Article history:

Received 16 July 2015

Received in revised form 6 November 2015

Accepted 16 November 2015

Available online 28 November 2015

Editor: L. Rolandi

ABSTRACT

We present results of a search for two hypothetical strange dibaryon states, i.e. the H-dibaryon and the possible $\bar{\Lambda}n$ bound state. The search is performed with the ALICE detector in central (0–10%) Pb–Pb collisions at $\sqrt{s_{NN}} = 2.76$ TeV, by invariant mass analysis in the decay modes $\bar{\Lambda}n \rightarrow \bar{d}\pi^+$ and H-dibaryon $\rightarrow \Lambda p\pi^-$. No evidence for these bound states is observed. Upper limits are determined at 99% confidence level for a wide range of lifetimes and for the full range of branching ratios. The results are compared to thermal, coalescence and hybrid UrQMD model expectations, which describe correctly the production of other loosely bound states, like the deuteron and the hypertriton.

© 2015 CERN for the benefit of the ALICE Collaboration. Published by Elsevier B.V. This is an open access article under the CC BY license (<http://creativecommons.org/licenses/by/4.0/>). Funded by SCOAP³.

1. Introduction

Particle production in Pb–Pb collisions at the Large Hadron Collider (LHC) has been extensively studied [1–3]. The observed production pattern is rather well described in equilibrium thermal models [4–7]. Within this approach, the chemical freeze-out temperature T_{chem} , the volume V and the baryo-chemical potential μ_B are the only three free parameters. Even loosely bound states such as the deuteron and hypertriton and their anti-particles have been observed [8–10] and their rapidity densities are properly described [11–17]. Consequently other loosely bound states¹ such as the H-dibaryon and the Λn are expected to be produced with corresponding yields.

The discovery of the H-dibaryon or the Λn bound state would be a breakthrough in hadron spectroscopy as it would imply the existence of a six-quark state and provide crucial information on the Λ -nucleon and Λ - Λ interaction. We consequently have started the investigation on the possible existence of such exotic bound states in pp and Pb–Pb collisions at the LHC. Searches for Λ -nucleon bound states in the Λp and Λn channels have been carried out (see Refs. [18–20]). The H-dibaryon, which is a hypothetical bound state of $uuddss$ ($\Lambda\Lambda$), was first predicted by Jaffe using a bag model approach [21]. Experimental searches have been undertaken since then, but no evidence for a signal was found (see [22,23] and the references therein). Recently, the STAR Collaboration investigated the Λ - Λ interaction through the measure-

ment of $\Lambda\Lambda$ correlations [24]; this and a theoretical analysis of these data [25] did not reveal a signal. Many theoretical investigations of the possible stability of the H-dibaryon have been carried out, but predicting binding energies in the order of MeV for masses of around $2 \text{ GeV}/c^2$ is extremely difficult and challenging [26–29].

Our approach is to search for such bound states in central Pb–Pb collisions at LHC energies where rapidity densities can be well predicted by thermal [16,17,30] and coalescence [31] models. The model predictions for rapidity densities of these particles are used and tested against the experimental results.

In this paper the analysis strategies for the searches of the $\bar{\Lambda}n \rightarrow \bar{d}\pi^+$ bound state and the H-dibaryon $\rightarrow \Lambda p\pi^-$ are presented. The analysis focuses on the $\bar{\Lambda}n$ bound state because production of anti-particles in the detector material is strongly suppressed and thus secondary contamination of the signal is reduced. For the H-dibaryon both the Λ and the p originate from secondary vertices where knock-out background is less likely. No search for the anti-H is performed yet, although it is assumed to be produced with equal yield but the measurement depends strongly on the absorption correction. We begin with a short introduction to the ALICE detector and a description of the particle identification technique used to identify the decay daughters and reconstruct invariant mass distributions. To assess the possible existence of these states we compare the experimental distributions with the model predictions.

2. Detector setup and data sample

The ALICE detector [32] is specifically designed to study heavy-ion collisions. The central barrel comprising the two main tracking detectors, the Inner Tracking System (ITS) [33] and the Time

* E-mail address: alice-publications@cern.ch.

¹ The expected masses of these states are some MeV below the sum of the mass of their constituents.

Projection Chamber (TPC) [34] is housed in a large solenoidal magnet providing a 0.5 T field. The detector pseudorapidity coverage is $|\eta| \leq 0.9$ over the full azimuth. An additional part of the central barrel are detectors in forward direction used mainly for triggering and centrality selection. The VZERO detectors, two scintillation hodoscopes, are placed on either side of the interaction point and cover the pseudorapidity regions of $2.8 < \eta < 5.1$ and $-3.7 < \eta < -1.7$. The centrality selection is based on the sum of the amplitudes measured in both detectors as described in [35] and [36].

The ITS consists of six cylindrical layers of three different types of silicon detectors. The innermost part comprises two silicon pixel (SPD) and two silicon drift detector (SDD) layers. The two outer layers are double-sided silicon microstrip detectors (SSD). Due to the precise space points provided by the ITS a high precision determination of the collision vertex is possible. Therefore, primary and secondary particles can be well separated, down to 100 μm precision at low transverse momentum ($p_{\text{T}} \approx 100 \text{ MeV}/c$).

The TPC is the main tracking detector of ALICE and surrounds the ITS. It has a cylindrical design with a diameter of $\approx 550 \text{ cm}$, an inner radius of 85 cm, an outer radius of 247 cm and an overall length in the beam direction of $\approx 510 \text{ cm}$. The 88 m^3 gas volume of the TPC is filled with a mixture of 85.7% Ne, 9.5% CO₂ and 4.8% N₂. When a charged particle is travelling through the TPC, it ionizes the gas along its path and electrons are released. Due to the uniform electric field along the z-axis (parallel to the beam axis and to the magnetic field) the electrons drift towards the end plates, where the electric signals are amplified and detected in 557 568 pads. These data are used to calculate a particle trajectory in the magnetic field and thus determine the track rigidity $\frac{p}{z}$ (the momentum p of the particle divided by its charge number z). The TPC is also used for particle identification via the energy deposit dE/dx measurement (see section 3).

A complete description of the performance of the ALICE sub-detectors in pp, p-Pb and Pb-Pb collisions can be found in [37].

The searches carried out and reported here are performed by analysing the data set of Pb-Pb collisions from 2011. In the described analyses we use 19.3×10^6 events with a centrality of 0–10%, determined by the aforementioned VZERO detectors from the previously mentioned campaign.

3. Particle identification

The precise Particle IDentification (PID) and continuous tracking from very low p_{T} (100 MeV/c) to moderately high p_{T} (20 GeV/c) is a unique feature of the ALICE detector at the LHC. The PID used in the analysis described in this letter takes advantage of two different techniques. The energy deposit (dE/dx) and rigidity are measured with the TPC for each reconstructed charged-particle trajectory. This allows the identification of all charged stable particles, from the lightest (electron) to the heaviest ones (anti-alpha). The energy deposit resolution of the TPC in central Pb-Pb collisions (investigated here) is around 7%. The corresponding particle separation power is demonstrated in Fig. 1. This technique was used in the following to identify the deuterons, protons and pions. The second method makes use of specific topologies from weak decays, which result in typical V^0 decay patterns. This is used here for the detection of the Λn bound state and the two V^0 decay patterns of the $\Lambda\Lambda$, namely for the Λ identification and the proton–pion decay vertex.

4. Analysis

The strategies of investigation for the two exotic bound states discussed here are quite similar. They both require the detection

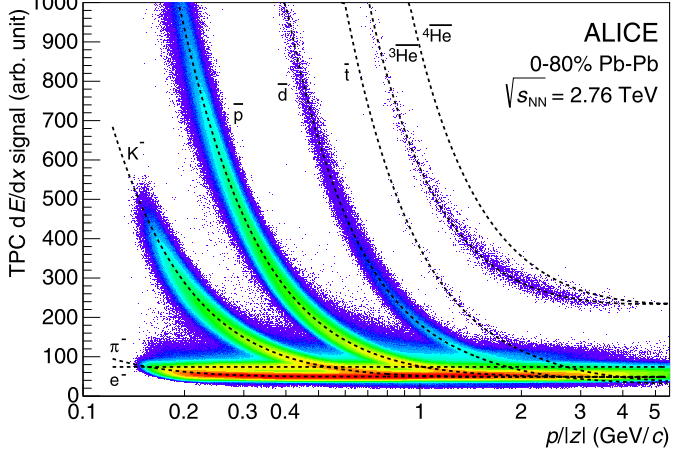


Fig. 1. TPC dE/dx spectrum for negative particles in a sample of three different trigger types (minimum bias, semi-central and central). The dashed lines are parametrisations of the Bethe–Bloch-formula [38–40] for the different particle species.

of a secondary vertex, which in one case is a pure V^0 and in the second a double V^0 decay pattern. We discuss them separately in the following sub-sections. First we describe briefly the common aspects of both analyses.

The tracks used in the analyses have to fulfil a set of selection criteria to ensure high tracking efficiency and dE/dx resolution. Each track was required to have at least 70 of up to 159 clusters in the TPC attached to it, with the (rather loose) requirement, that the χ^2 of the momentum fit is smaller than 5 per cluster. Tracks with kinks due to weak decays of kaons and pions are rejected. To achieve final precision the accepted tracks are refit while the track finding algorithm is run inwards, outwards and inwards again (for more details on the ALICE tracking see [37] and section 5 of [41]).

V^0 decays are determined by two (or more) tracks which are emitted from a secondary vertex and which might come close to each other (the minimum distance is called Distance-of-Closest-Approach DCA) while each of the tracks has a certain minimum distance (DCA of the track to a vertex) to the primary vertex. A powerful selection criterion for detecting proper V^0 candidates is the restriction of the pointing angle, namely the angle between the reconstructed flight-line and the reconstructed momentum of the V^0 particle. More details of the secondary vertex reconstruction can be found in [3,37,41], where also the clear and effective identification of Λ baryons is displayed using the aforementioned technique. The selection criteria, described below, are optimised using a Monte Carlo set where the simulated exotic bound states are assumed to live as long as a free Λ baryon. This is a reasonable assumption for all strange dibaryons, which are expected to live around $2\text{--}4 \times 10^{-10} \text{ s}$ [42–44] in the regions of binding energies investigated here.

4.1. $\overline{\Lambda}n$ bound state

In analogy to recent hypertriton measurements [8,9] we focus here on the expected two-body decay $\overline{\Lambda}n \rightarrow \bar{d}\pi^+$. For the data analysis the following strategy is used: first displaced vertices are identified using ITS and TPC information. In a second step the negative track of the V^0 candidate is identified as an anti-deuteron via the TPC dE/dx information. If the second daughter is identified as a pion, the invariant mass of the pair is reconstructed. Both particles are required to lie within a 3 standard deviations (σ) band of the expected Bethe–Bloch lines of the corresponding particles.

Table 1
Selection criteria for $\overline{\Lambda}\eta$ analysis.

Selection criterion	Value
<i>Track selection criteria</i>	
Tracks with kinks	rejected
Number of clusters in TPC	$n_{\text{cl}} > 70$
Track quality	$\chi^2/\text{cluster} < 5$
Acceptance in pseudorapidity	$ \eta < 0.9$
Acceptance in rapidity	$ y < 1$
<i>V^0 and kinematic selection criteria</i>	
Pointing angle	$\Theta < 0.045 \text{ rad}$
DCA between the V^0 daughters	$\text{DCA} < 0.3 \text{ cm}$
Momentum p_{tot} of the anti-deuteron	$p_{\text{tot}} > 0.2 \text{ GeV}/c$
Energy deposit dE/dx anti-deuteron	$dE/dx > 110$ (from Fig. 1)
PID cut for daughters	$\pm 3\sigma$ (TPC)

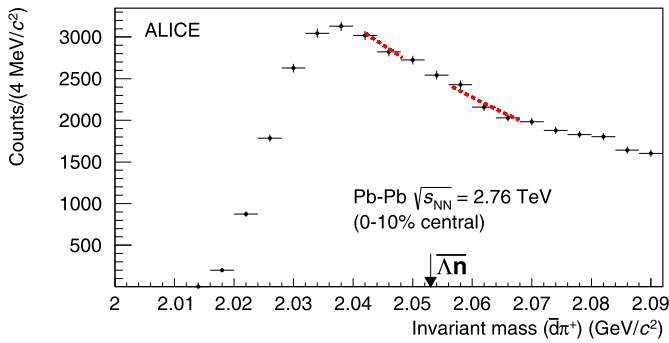


Fig. 2. Invariant mass distribution for $\bar{d}\pi^+$ for the Pb-Pb data corresponding to 19.3×10^6 central events. The arrow indicates the sum of the mass of the constituents ($\overline{\Lambda}\eta$) of the assumed bound state. A signal for the bound state is expected in the region below this sum. The dashed line represents an exponential fit outside the expected signal region to estimate the background.

To identify the secondary vertex the two daughter tracks have to have a DCA smaller than 0.3 cm. Another condition is that the maximum pointing angle is smaller than 0.045 rad (see description above). Deuterons are cleanly identified in the rigidity region of 400 MeV/c to 1.75 GeV/c. To limit contamination from other particle species, the dE/dx has to be above 110 units of the TPC signal, shown in Fig. 1.

The selection criteria are summarised in Table 1. The resulting invariant mass distribution, reflecting the kinematic range of identified daughter tracks, is displayed in Fig. 2.

4.2. H-dibaryon

The search for the H-dibaryon is performed in the decay channel $H \rightarrow \Lambda p\pi^-$, with a mass lying in the range $2.200 \text{ GeV}/c^2 < m_H < 2.231 \text{ GeV}/c^2$ (see Fig. 3). The analysis strategy for the H-dibaryon is similar as for the $\overline{\Lambda}\eta$ bound state described above, except that here a second V^0 -type decay particle is involved.

One V^0 candidate originating from the H-dibaryon decay vertex has to be identified as a Λ decaying into a proton and a pion. In addition another V^0 decay pattern reconstructed from a proton and a pion is required to be found at the decay vertex of the H-dibaryon. First the invariant mass of the Λ is reconstructed and then the candidates in the invariant mass window of $1.111 \text{ GeV}/c^2 < m_\Lambda < 1.120 \text{ GeV}/c^2$ are combined with the four-vectors of the proton and pion at the decay vertex. A 3σ dE/dx cut in the TPC is used to identify the protons and the pions for both the Λ candidate and the V^0 topology at the H-dibaryon decay vertex.

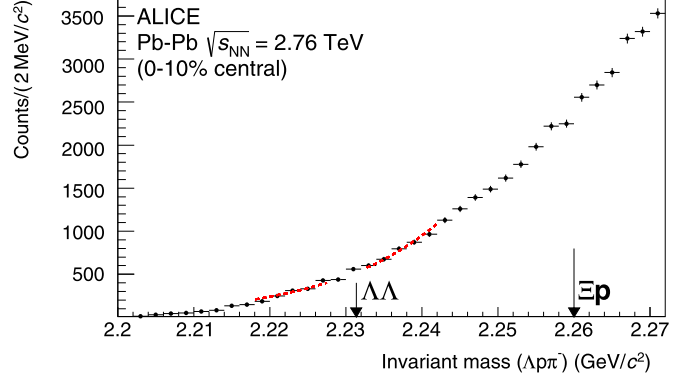


Fig. 3. Invariant mass distribution for $\Lambda p\bar{\pi}$ for the Pb-Pb data corresponding to 19.3×10^6 central events. The left arrow indicates the sum of the masses of the constituents ($\Lambda\Lambda$) of the possible bound state. A signal for the bound state is expected in the region below this sum. For the speculated resonant state a signal is expected between the $\Lambda\Lambda$ and the Ξp (indicated by the right arrow) thresholds. The dashed line is an exponential fit to estimate the background.

Table 2
Selection criteria used for $\Lambda\Lambda$ (H-dibaryon) analysis.

Selection criterion	Value
<i>Track selection criteria</i>	
Tracks with kinks	rejected
Number of clusters in TPC	$n_{\text{cl}} > 80$
Track quality	$\chi^2/\text{cluster} < 5$
Acceptance in pseudorapidity	$ \eta < 0.9$
Acceptance in rapidity	$ y < 1$
<i>V^0 selection criteria</i>	
DCA V^0 daughters	$\text{DCA} < 1 \text{ cm}$
DCA positive V^0 daughter – H decay vertex	$\text{DCA} > 2 \text{ cm}$
DCA negative V^0 daughter – H decay vertex	$\text{DCA} > 2 \text{ cm}$
<i>Kinematic selection criteria</i>	
DCA positive H daughter – primary vertex	$\text{DCA} > 2 \text{ cm}$
DCA negative H daughter – primary vertex	$\text{DCA} > 2 \text{ cm}$
DCA H daughters	$\text{DCA} < 1 \text{ cm}$
Pointing angle of H	$\Theta < 0.05 \text{ rad}$
PID cut for daughters	$\pm 3\sigma$ (TPC)
Λ mass window	$\pm 3\sigma$

To cope with the huge background caused by primary and secondary pions additional selection criteria have to be applied. Each track is required to be at least 2 cm away from the primary vertex and the tracks combined to a V^0 are required to have a minimum distance below 1 cm. The pointing angle is required to be below 0.05 rad. All selection criteria are summarised in Table 2. The resulting invariant mass is shown in Fig. 3. The shape of the invariant mass distribution is caused by the kinematic range of the identified daughter tracks.

5. Systematics and absorption correction

Monte Carlo samples have been produced to estimate the efficiency for the detection of the $\overline{\Lambda}\eta$ bound state and the H-dibaryon. The kinematical distributions of the hypothetical bound states were generated uniformly in rapidity y and in transverse momentum p_T . In order to deal with the unknown lifetime, different decay lengths are investigated, ranging from 4 cm up to 3 m. The lower limit is determined by the secondary vertex finding efficiency and the upper limit by the requirement that there is a significant probability for decays inside the TPC² (the final accep-

² For the H-dibaryon there is also a theoretical maximal decay length calculated for the investigated decay channel [45].

tance \times efficiency drops down to 1% for the $\bar{\Lambda}n$ and 10^{-3} for the H-dibaryon). The shape of transverse momentum spectra in heavy-ion collisions is described well by the blast-wave approach, with radial flow parameter $\langle\beta\rangle$ and kinetic freeze-out temperature T_{kin} as in [46]. The true shape of the p_T spectrum is also not known, therefore it is estimated from the extrapolation of blast-wave fits to deuterons and ^3He spectra at the same energy [10]. To obtain final efficiencies, the resulting blast-wave distributions constructed for the exotic bound states are normalised to unity and convoluted with the correction factors (efficiency \times acceptance).

Typical values of the final efficiency are of the order of a few percent assuming the lifetime of the free Λ . The uncertainty in the shape of the p_T distributions is the main source of systematic error. Blast-wave fits of deuteron and ^3He spectra are employed to explore the range of systematic uncertainties. Analyses of these results lead to a systematic uncertainty in the overall yield of around 25%.

Other systematic uncertainties are estimated by varying the cuts described in Table 1 and Table 2 within the limits consistent with the detector resolution. The contributions of these systematic uncertainties are typically found to be in the percent range. The combination of the different sources leads to a global systematic uncertainty of around 30% for both analyses, when all uncertainties are added in quadrature.

For the $\bar{\Lambda}n$ bound state analysis the possible absorption of the anti-deuterons and the bound state itself when crossing material has to be taken into account. For this, the same procedure as used for the anti-hypertriton analysis [9] is utilised. The absorption correction ranges from 3 to 40% (depending on the lifetime of the $\bar{\Lambda}n$ bound state, which determines the amount of material crossed) with an overall uncertainty of 7%.

6. Results

No significant signal in the invariant mass distributions has been observed for both cases, as visible from Fig. 2 and Fig. 3.³ The shape of the invariant mass distribution of $d\pi^+$ is of purely kinematic origin, reflecting the momentum distribution of the particles used. The selection criteria listed in Table 1 are tuned to select secondary decays. The secondary anti-deuterons involved in the analysis originate mainly from two sources: The first and dominating source are daughters from three-body decays of the anti-hypertriton (${}^3\bar{\Lambda}\text{H} \rightarrow \bar{d}\bar{p}\pi^+$ and ${}^3\bar{\Lambda}\text{H} \rightarrow \bar{d}\bar{n}\pi^0$) where the other decay daughters are not detected. The invariant mass spectrum is obtained by combining these anti-deuterons with pions generated in the collision. The second source is due to prompt anti-deuterons which are incorrectly labelled as displaced, because they have such low momenta that the DCA resolution of these tracks is not sufficient to separate primary from secondary particles.

Since no signal in the invariant mass distributions is observed upper limits are estimated. For the estimation of upper limits for the rapidity density dN/dy the method discussed in [47] is utilised. In particular, we apply the software package *TRolke* as implemented in *ROOT* [48]. This method needs as input mass and experimental width (3σ) of the hypothetical bound states. The observed counts are therefore compared to a smooth background as given by an exponential fit outside the signal region (as indicated by the line in Fig. 2 and Fig. 3). For both candidates $\bar{\Lambda}n$ and H-dibaryon we assume a binding energy of 1 MeV. The width is determined by the experimental resolution and obtained from

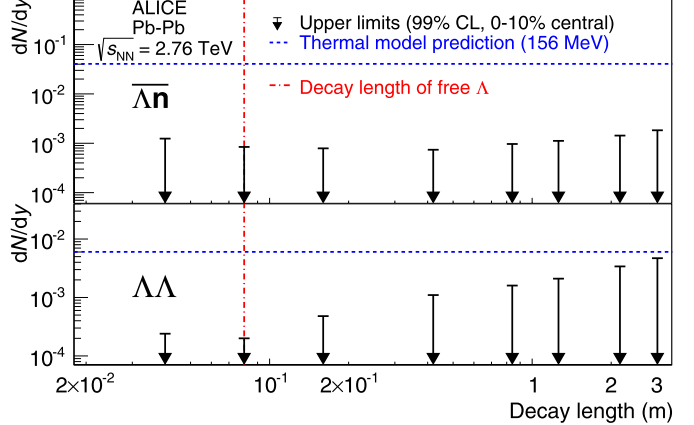


Fig. 4. Upper limit of the rapidity density shown for the $\bar{\Lambda}n$ bound state in the upper panel and for the H-dibaryon in the lower panel. Here a branching ratio of 64% was used for the H-dibaryon and a branching ratio of 54% for the $\bar{\Lambda}n$ bound state. The horizontal (dashed) lines indicate the expectation of the thermal model with a temperature of 156 MeV. The vertical line shows the lifetime of the free Λ baryon. (For interpretation of the references to colour in this figure, the reader is referred to the web version of this article.)

Monte Carlo simulations. In addition, the final efficiency which is discussed in section 5 is required. Further, values of branching ratios of the assumed bound states are needed. These depend strongly on the binding energy. With a 1 MeV binding energy for the $\bar{\Lambda}n$ bound state the branching ratio in the $\bar{d} + \pi^+$ decay channel is expected to be 54% [49]. The branching ratio for a 1 MeV or less bound H-dibaryon decaying into $\Lambda p\pi^-$ is predicted to be 64%, see [44].

The resulting upper limits, for 99% CL, are shown in Fig. 4 as a function of the different lifetimes; for the $\bar{\Lambda}n$ bound state in the upper panel and for the H-dibaryon in the lower panel. These upper limits include systematic uncertainties. For the $\bar{\Lambda}n$ the absorption corrections are also considered in the figure, which causes the upper limits to be shifted upwards.

The obtained upper limits can now be compared to model predictions. The rapidity densities dN/dy from a thermal model prediction for a chemical freeze-out temperature of, for example, 156 MeV, are $dN/dy = 4.06 \times 10^{-2}$ for the $\bar{\Lambda}n$ bound state and $dN/dy = 6.03 \times 10^{-3}$ for the H-dibaryon [16]. These values are indicated with the (blue) dashed lines in Fig. 4. For the investigated range of lifetimes the upper limit of the $\bar{\Lambda}n$ bound state is at least a factor 20 below this prediction. For the H-dibaryon the upper limits depend more strongly on the lifetime since it has a different decay topology and all four final state tracks have to be reconstructed. The upper limit is a factor of 20 below the thermal model prediction for the lifetime of the free Λ and becomes less stringent at higher lifetimes since the detection efficiency becomes small. For a lifetime of 10^{-8} s, corresponding to a decay length of 3 m, the difference between model and upper limit reduces to a factor two.

In order to take the uncertainties in the branching ratio into account, we plot in Fig. 5 the products of the upper limit of the rapidity density times the branching ratio together with several theory predictions [16,30,31,50]. The curves are obtained using the value for the Λ -lifetime of Fig. 4.

The (red) arrows in the figures indicate the branching ratio from the theory predictions [44,49]. The obtained upper limits are a factor of more than 5 below all theory predictions for a branching ratio of at least 5% for the $\bar{\Lambda}n$ bound state and at least 20% for the H-dibaryon.

³ Note that a hypothetical H-dibaryon with a mass above the Ξp threshold would not be observable in the present analysis.

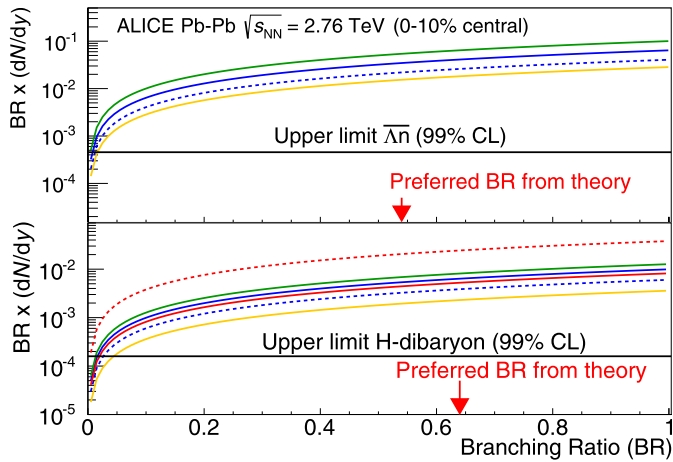


Fig. 5. Experimentally determined upper limit, under the assumption of the lifetime of a free Λ . In the upper panel shown for the $\bar{\Lambda}n$ bound state and for the H-dibaryon in the lower panel. It includes 30% systematic uncertainty for each particle and 6% correction for absorption with an uncertainty of 7% for the $\bar{\Lambda}n$ bound state. The theory lines are drawn for different theoretical branching ratios (BR) in blue for the equilibrium thermal model from [16] for two temperatures (164 MeV the full line and 156 MeV the dashed line), in green the non-equilibrium thermal model from [30] and in yellow the predictions from a hybrid UrQMD calculation [50]. The H-dibaryon is also compared with predictions from coalescence models, where the full red line visualises the prediction assuming quark coalescence and the dashed red line corresponds to hadron coalescence [31]. (For interpretation of the references to colour in this figure legend, the reader is referred to the web version of this article.)

7. Discussion

The limits obtained on the rapidity density of the investigated exotic compound objects are found to be more than one order of magnitude below the expectations of particle production models, when using a realistic branching ratio and a reasonable lifetime. It has to be noted that simultaneously, a clear signal was observed for the very loosely bound hypertriton (binding energy < 150 keV) for which production yields have been measured [9]. These yields along with those of nuclei $A = 2, 3, 4$ agree well with the predictions of the thermal model discussed above and decrease with each additional baryon number by roughly a factor 300. One would therefore assume that the yield of the $\bar{\Lambda}n$, if such particle existed, should also be predicted by this model and with a value for the rapidity density of about a factor 300 higher than the measured hypertriton yield. Similar considerations hold for the H-dibaryon.

8. Conclusion

A search is reported for the existence of loosely bound strange dibaryons $\Lambda\Lambda$ and $\bar{\Lambda}n$ whose possible existence has been discussed widely in the literature. No signals are observed. On the other hand, loosely bound objects with baryon number $A = 3$ such as the hypertriton have been measured in the same data sample. The yields of nuclei [10] and of the hypertriton [9] are quantitatively understood within a thermal model calculation. The present analysis provides stringent upper limits at 99% confidence level for the production of H-dibaryon and Λn bound state, in general significantly below the thermal model predictions. The upper limits are obtained for different lifetimes. The values are well below the model predictions when realistic branching ratios and reasonable lifetimes are assumed. Thus, our results do not support the existence of the H-dibaryon and the Λn bound state.

Acknowledgements

We thank S. Beane, M. Petráň, J. Schaffner-Bielich and J. Steinheimer for useful correspondence.

The ALICE Collaboration would like to thank all its engineers and technicians for their invaluable contributions to the construction of the experiment and the CERN accelerator teams for the outstanding performance of the LHC complex. The ALICE Collaboration gratefully acknowledges the resources and support provided by all Grid centres and the Worldwide LHC Computing Grid (WLCG) Collaboration. The ALICE Collaboration acknowledges the following funding agencies for their support in building and running the ALICE detector: State Committee of Science, World Federation of Scientists (WFS) and Swiss Fonds Kidagan, Armenia, Conselho Nacional de Desenvolvimento Científico e Tecnológico (CNPq), Financiadora de Estudos e Projetos (FINEP), Fundação de Amparo à Pesquisa do Estado de São Paulo (FAPESP); National Natural Science Foundation of China (NSFC), the Chinese Ministry of Education (CMOE) and the Ministry of Science and Technology of the People's Republic of China (MSTC); Ministry of Education and Youth of the Czech Republic; Danish Natural Science Research Council, the Carlsberg Foundation and the Danish National Research Foundation; The European Research Council under the European Community's Seventh Framework Programme; Helsinki Institute of Physics and the Academy of Finland; French CNRS-IN2P3, the 'Region Pays de Loire', 'Region Alsace', 'Region Auvergne' and CEA, France; German Bundesministerium für Bildung, Wissenschaft, Forschung und Technologie (BMBF) and the Helmholtz Association; General Secretariat for Research and Technology, Ministry of Development, Greece; Hungarian Országos Tudományos Kutatási Alap (OTKA) and National Office for Research and Technology (NKTH); Department of Atomic Energy and Department of Science and Technology of the Government of India; Istituto Nazionale di Fisica Nucleare (INFN) and Centro Fermi – Museo Storico della Fisica e Centro Studi e Ricerche "Enrico Fermi", Italy; MEXT Grant-in-Aid for Specially Promoted Research, Japan; Joint Institute for Nuclear Research, Dubna; National Research Foundation of Korea (NRF); Consejo Nacional de Ciencia y Tecnología (CONACYT), Dirección General de Asuntos del Personal Académico (DGAPA), México, Amerique Latine Formation académique – European Commission (ALFA-EC) and the EPLANET Program (European Particle Physics Latin American Network); Stichting voor Fundamenteel Onderzoek der Materie (FOM) and the Nederlandse Organisatie voor Wetenschappelijk Onderzoek (NWO), Netherlands; Research Council of Norway (NFR); National Science Centre, Poland; Ministry of National Education/Institute for Atomic Physics and National Council of Scientific Research in Higher Education (CNCSI-UEFISCDI), Romania; Ministry of Education and Science of the Russian Federation, Russian Academy of Sciences, Russian Federal Agency of Atomic Energy, Russian Federal Agency for Science and Innovations and The Russian Foundation for Basic Research; Ministry of Education of Slovakia; Department of Science and Technology, Republic of South Africa; Centro de Investigaciones Energéticas, Medioambientales y Tecnológicas (CIEMAT), E-Infrastructure shared between Europe and Latin America (EELA), Ministerio de Economía y Competitividad (MINECO) of Spain, Xunta de Galicia (Conselería de Educación), Centro de Aplicaciones Tecnológicas y Desarrollo Nuclear (CEADEN), Cubaenergía, Cuba, and IAEA (International Atomic Energy Agency); Swedish Research Council (VR) and Knut and Alice Wallenberg Foundation (KAW); Ukraine Ministry of Education and Science; United Kingdom Science and Technology Facilities Council (STFC); The United States Department of Energy, the United States National Science Foundation, the State of Texas, and the State of

Ohio; Ministry of Science, Education and Sports of Croatia and Unity through Knowledge Fund, Croatia; Council of Scientific and Industrial Research (CSIR), New Delhi, India.

References

- [1] ALICE Collaboration, B. Abelev, et al., Pion, kaon, and proton production in central Pb–Pb collisions at $\sqrt{s_{NN}} = 2.76$ TeV, Phys. Rev. Lett. 109 (2012) 252301.
- [2] ALICE Collaboration, B. Abelev, et al., Centrality dependence of π , K, p production in Pb–Pb collisions at $\sqrt{s_{NN}} = 2.76$ TeV, Phys. Rev. C 88 (2013) 044910.
- [3] ALICE Collaboration, B. Abelev, et al., K_s^0 and Λ production in Pb–Pb collisions at $\sqrt{s_{NN}} = 2.76$ TeV, Phys. Rev. Lett. 111 (2013) 222301.
- [4] P. Braun-Munzinger, K. Redlich, J. Stachel, Invited review, in: R.C. Hwa, X.N. Wang (Eds.), Quark Gluon Plasma, vol. 3, World Scientific Publishing, 2004, arXiv:nucl-th/0304013.
- [5] F. Becattini, J. Manninen, M. Gaździcki, Energy and system size dependence of chemical freeze-out in relativistic nuclear collisions, Phys. Rev. C 73 (2006) 044905.
- [6] A. Andronic, P. Braun-Munzinger, J. Stachel, Thermal hadron production in relativistic nuclear collisions: the hadron mass spectrum, the horn, and the QCD phase transition, Phys. Lett. B 673 (2009) 142, Erratum, Phys. Lett. B 678 (2009) 516.
- [7] J. Cleymans, K. Redlich, Chemical and thermal freeze-out parameters from 1A to 200A GeV, Phys. Rev. C 60 (1999) 054908.
- [8] STAR Collaboration, B.I. Abelev, et al., Observation of an antimatter hypernucleus, Science 328 (2010) 58.
- [9] ALICE Collaboration, J. Adam, et al., ${}^3_A\text{H}$ and ${}^3_A\overline{\text{H}}$ production in Pb–Pb collisions at $\sqrt{s_{NN}} = 2.76$ TeV, arXiv:1506.08453 [nucl-ex].
- [10] ALICE Collaboration, J. Adam, et al., Production of light nuclei and anti-nuclei in pp and Pb–Pb collisions at LHC energies, arXiv:1506.08951 [nucl-ex].
- [11] P. Braun-Munzinger, J. Stachel, Production of strange clusters and strange matter in nucleus–nucleus collisions at the AGS, J. Phys. G 21 (1995) L17.
- [12] P. Braun-Munzinger, J. Stachel, Particle ratios, equilibration and the QCD phase boundary, J. Phys. G 28 (2002) 1971.
- [13] A. Andronic, P. Braun-Munzinger, J. Stachel, H. Stöcker, Production of light nuclei, hypernuclei and their antiparticles in relativistic nuclear collisions, Phys. Lett. B 697 (2011) 203.
- [14] J. Cleymans, S. Kabana, I. Kraus, H. Oeschler, K. Redlich, N. Sharma, Antimatter production in proton–proton and heavy-ion collisions at ultrarelativistic energies, Phys. Rev. C 84 (2011) 054916.
- [15] A. Andronic, P. Braun-Munzinger, K. Redlich, J. Stachel, The statistical model in Pb–Pb collisions at the LHC, Nucl. Phys. A 904–905 (2013) 535c.
- [16] J. Stachel, A. Andronic, P. Braun-Munzinger, K. Redlich, Confronting LHC data with the statistical hadronization model, J. Phys. Conf. Ser. 509 (2014) 012019.
- [17] J. Steinheimer, K. Gudima, A. Botvina, I. Mishustin, M. Bleicher, H. Stöcker, Hypernuclei, dibaryon and antinuclei production in high energy heavy ion collisions: thermal production vs. coalescence, Phys. Lett. B 714 (2012) 85.
- [18] HiRes Collaboration, A. Budzanowski, et al., High resolution study of the p final state interaction in the reaction $p + p \rightarrow K^+ + (\Lambda p)$, Phys. Lett. B 687 (2010) 31.
- [19] HiRes Collaboration, A. Budzanowski, et al., Upper limits for a narrow resonance in the reaction $p + p \rightarrow K^+ + (\Lambda p)$, Phys. Rev. D 84 (2011) 032002.
- [20] HypHI Collaboration, C. Rappold, et al., Search for evidence of ${}^3_A\text{n}$ by observing $d + \pi^-$ and $t + \pi^-$ final states in the reaction of ${}^6\text{Li} + {}^{12}\text{C}$ at 2A GeV, Phys. Rev. C 88 (2013) 041001.
- [21] R.L. Jaffe, Perhaps stable dihyperon, Phys. Rev. Lett. 38 (1977) 195, Erratum, Phys. Rev. Lett. 38 (1977) 617.
- [22] R.E. Chrien, H particle searches at Brookhaven, Nucl. Phys. A 629 (1998) 388c.
- [23] BELLE Collaboration, B.H. Kim, et al., Search for an H-dibaryon with a mass near $2m_\Lambda$ in $\Upsilon(1S)$ and $\Upsilon(2S)$ decays, Phys. Rev. Lett. 110 (2013) 222002.
- [24] STAR Collaboration, L. Adamczyk, et al., The $\Lambda\Lambda$ correlation function in Au + Au collisions at $\sqrt{s_{NN}} = 200$ GeV, Phys. Rev. Lett. 114 (2015) 022301.
- [25] K. Morita, T. Furumoto, A. Ohnishi, Lambda–Lambda interaction from relativistic heavy-ion collisions, arXiv:1408.6682v1 [nucl-th].
- [26] NPLQCD Collaboration, S.R. Beane, et al., Evidence for a bound H dibaryon from lattice QCD, Phys. Rev. Lett. 106 (2011) 162001.
- [27] HALQCD Collaboration, T. Inoue, et al., Bound dibaryon in flavor SU(3) limit of lattice QCD, Phys. Rev. Lett. 106 (2011) 162002.
- [28] P. Shanahan, A.W. Thomas, R.D. Young, Mass of the H dibaryon, Phys. Rev. Lett. 107 (2011) 092004.
- [29] J. Haidenbauer, U.-G. Meißner, To bind or not to bind: the H-dibaryon in light of chiral effective field theory, Phys. Lett. B 706 (2011) 100.
- [30] M. Petráň, calculation based on [51] and [52], 2013.
- [31] ExHIC Collaboration, S. Cho, et al., Exotic hadrons in heavy ion collisions, Phys. Rev. C 84 (2011) 064910.
- [32] ALICE Collaboration, K. Aamodt, et al., The ALICE experiment at the CERN LHC, J. Instrum. 3 (2008) S08002.
- [33] ALICE Collaboration, K. Aamodt, et al., Alignment of the ALICE Inner Tracking System with cosmic-ray tracks, J. Instrum. 5 (2010) P03003.
- [34] J. Alme, et al., The ALICE TPC, a large 3-dimensional tracking device with fast readout for ultra-high multiplicity events, Nucl. Instrum. Methods A 622 (2010) 316.
- [35] ALICE Collaboration, K. Aamodt, et al., Centrality dependence of the charged-particle multiplicity density at midrapidity in Pb–Pb collisions at $\sqrt{s_{NN}} = 2.76$ TeV, Phys. Rev. Lett. 106 (2011) 032301.
- [36] ALICE Collaboration, B. Abelev, et al., Centrality determination of Pb–Pb collisions at $\sqrt{s_{NN}} = 2.76$ TeV with ALICE, Phys. Rev. C 88 (2013) 044909.
- [37] ALICE Collaboration, B. Abelev, et al., Performance of the ALICE experiment at the CERN LHC, Int. J. Mod. Phys. A 29 (2014) 1430044.
- [38] H. Bethe, Bremsformel für Elektronen relativistischer Geschwindigkeit, Z. Phys. 76 (1932) 293.
- [39] F. Bloch, Zur Bremsung rasch bewegter Teilchen beim Durchgang durch Materie, Ann. Phys. 408 (1933) 285.
- [40] W. Blum, W. Riegler, L. Rolandi, Particle Detection with Drift Chambers, Springer Publishing, 2008.
- [41] ALICE Collaboration, B. Alessandro, et al., ALICE: physics performance report, volume II, J. Phys. G, Nucl. Part. Phys. 32 (2006) 1295.
- [42] M.I. Krivoruchenko, M.G. Shchepkin, Dilambda decays, Sov. J. Nucl. Phys. 36 (1982) 769.
- [43] J. Schaffner, C.B. Dover, A. Gal, C. Greiner, H. Stöcker, Strange hadronic matter, Phys. Rev. Lett. 71 (1993) 1328.
- [44] J. Schaffner-Bielich, R. Mattiello, H. Sorge, Dibaryons with strangeness: their weak nonleptonic decay using SU(3) symmetry and how to find them in relativistic heavy-ion collisions, Phys. Rev. Lett. 84 (2000) 4305.
- [45] J. Donoghue, E. Golowich, B. Holstein, Weak decays of the h dibaryon, Phys. Rev. D 34 (1986) 3434.
- [46] ALICE Collaboration, B. Abelev, et al., Centrality dependence of π , K, p production in Pb–Pb collisions at $\sqrt{s_{NN}} = 2.76$ TeV, Phys. Rev. C 88 (2013) 044910.
- [47] W.A. Rolke, A.M. López, J. Conrad, Limits and confidence intervals in the presence of nuisance parameters, Nucl. Instrum. Methods A 551 (2005) 493.
- [48] R. Brun, F. Rademakers, ROOT – an object oriented data analysis framework, in: Proceedings AIHENP'96 Workshop, Lausanne, Sep. 1996, Nucl. Instrum. Methods A 389 (1997) 81, see also <http://root.cern.ch>.
- [49] J. Schaffner-Bielich, calculation based on [44], 2012.
- [50] J. Steinheimer, calculation based on [17], 2013.
- [51] G. Torrieri, S. Steinke, W. Broniowski, W. Florkowski, J. Letessier, J. Rafelski, SHARE: statistical hadronization with resonances, Comput. Phys. Commun. 167 (2005) 229.
- [52] G. Torrieri, S. Jeon, J. Letessier, J. Rafelski, SHAREv2: fluctuations and a comprehensive treatment of decay feed-down, Comput. Phys. Commun. 175 (2006) 635.

ALICE Collaboration

J. Adam ³⁹, D. Adamová ⁸², M.M. Aggarwal ⁸⁶, G. Aglieri Rinella ³⁶, M. Agnello ¹¹⁰, N. Agrawal ⁴⁷, Z. Ahammed ¹³⁰, I. Ahmed ¹⁶, S.U. Ahn ⁶⁷, I. Aimo ^{93,110}, S. Aiola ¹³⁵, M. Ajaz ¹⁶, A. Akindinov ⁵⁷, S.N. Alam ¹³⁰, D. Aleksandrov ⁹⁹, B. Alessandro ¹¹⁰, D. Alexandre ¹⁰¹, R. Alfaro Molina ⁶³, A. Alici ^{104,12}, A. Alkin ³, J. Alme ³⁷, T. Alt ⁴², S. Altinpinar ¹⁸, I. Altsybeev ¹²⁹, C. Alves Garcia Prado ¹¹⁸, C. Andrei ⁷⁷, A. Andronic ⁹⁶, V. Anguelov ⁹², J. Anielski ⁵³, T. Antićić ⁹⁷, F. Antinori ¹⁰⁷, P. Antonioli ¹⁰⁴, L. Aphecetche ¹¹², H. Appelshäuser ⁵², S. Arcelli ²⁸, N. Armesto ¹⁷, R. Arnaldi ¹¹⁰, T. Aronsson ¹³⁵, I.C. Arsene ²², M. Arslandok ⁵², A. Augustinus ³⁶, R. Averbeck ⁹⁶, M.D. Azmi ¹⁹, M. Bach ⁴², A. Badalà ¹⁰⁶, Y.W. Baek ⁴³, S. Bagnasco ¹¹⁰, R. Bailhache ⁵², R. Bala ⁸⁹, A. Baldissari ¹⁵, M. Ball ⁹¹, F. Baltasar Dos Santos Pedrosa ³⁶, R.C. Baral ⁶⁰, A.M. Barbano ¹¹⁰, R. Barbera ²⁹, F. Barile ³³,

- G.G. Barnaföldi ¹³⁴, L.S. Barnby ¹⁰¹, V. Barret ⁶⁹, P. Bartalini ⁷, J. Bartke ¹¹⁵, E. Bartsch ⁵², M. Basile ²⁸, N. Bastid ⁶⁹, S. Basu ¹³⁰, B. Bathen ⁵³, G. Batigne ¹¹², A. Batista Camejo ⁶⁹, B. Batyunya ⁶⁵, P.C. Batzing ²², I.G. Bearden ⁷⁹, H. Beck ⁵², C. Bedda ¹¹⁰, N.K. Behera ^{48,47}, I. Belikov ⁵⁴, F. Bellini ²⁸, H. Bello Martinez ², R. Bellwied ¹²⁰, R. Belmont ¹³³, E. Belmont-Moreno ⁶³, V. Belyaev ⁷⁵, G. Bencedi ¹³⁴, S. Beole ²⁷, I. Berceanu ⁷⁷, A. Bercuci ⁷⁷, Y. Berdnikov ⁸⁴, D. Berenyi ¹³⁴, R.A. Bertens ⁵⁶, D. Berzana ^{36,27}, L. Betev ³⁶, A. Bhasin ⁸⁹, I.R. Bhat ⁸⁹, A.K. Bhati ⁸⁶, B. Bhattacharjee ⁴⁴, J. Bhom ¹²⁶, L. Bianchi ^{27,120}, N. Bianchi ⁷¹, C. Bianchin ^{133,56}, J. Bielčík ³⁹, J. Bielčíková ⁸², A. Bilandzic ⁷⁹, S. Biswas ⁷⁸, S. Bjelogrlic ⁵⁶, F. Blanco ¹⁰, D. Blau ⁹⁹, C. Blume ⁵², F. Bock ^{73,92}, A. Bogdanov ⁷⁵, H. Bøggild ⁷⁹, L. Boldizsár ¹³⁴, M. Bombara ⁴⁰, J. Book ⁵², H. Borel ¹⁵, A. Borissov ⁹⁵, M. Borri ⁸¹, F. Bossú ⁶⁴, M. Botje ⁸⁰, E. Botta ²⁷, S. Böttger ⁵¹, P. Braun-Munzinger ⁹⁶, M. Bregant ¹¹⁸, T. Breitner ⁵¹, T.A. Broker ⁵², T.A. Browning ⁹⁴, M. Broz ³⁹, E.J. Brucken ⁴⁵, E. Bruna ¹¹⁰, G.E. Bruno ³³, D. Budnikov ⁹⁸, H. Buesching ⁵², S. Bufalino ^{36,110}, P. Buncic ³⁶, O. Busch ⁹², Z. Buthelezi ⁶⁴, J.T. Buxton ²⁰, D. Caffarri ^{36,30}, X. Cai ⁷, H. Caines ¹³⁵, L. Calero Diaz ⁷¹, A. Caliva ⁵⁶, E. Calvo Villar ¹⁰², P. Camerini ²⁶, F. Carena ³⁶, W. Carena ³⁶, J. Castillo Castellanos ¹⁵, A.J. Castro ¹²³, E.A.R. Casula ²⁵, C. Cavicchioli ³⁶, C. Ceballos Sanchez ⁹, J. Cepila ³⁹, P. Cerello ¹¹⁰, B. Chang ¹²¹, S. Chapeland ³⁶, M. Chartier ¹²², J.L. Charvet ¹⁵, S. Chattopadhyay ¹³⁰, S. Chattopadhyay ¹⁰⁰, V. Chelnokov ³, M. Cherney ⁸⁵, C. Cheshkov ¹²⁸, B. Cheynis ¹²⁸, V. Chibante Barroso ³⁶, D.D. Chinellato ¹¹⁹, P. Chochula ³⁶, K. Choi ⁹⁵, M. Chojnacki ⁷⁹, S. Choudhury ¹³⁰, P. Christakoglou ⁸⁰, C.H. Christensen ⁷⁹, P. Christiansen ³⁴, T. Chujo ¹²⁶, S.U. Chung ⁹⁵, C. Cicalo ¹⁰⁵, L. Cifarelli ^{12,28}, F. Cindolo ¹⁰⁴, J. Cleymans ⁸⁸, F. Colamaria ³³, D. Colella ³³, A. Collu ²⁵, M. Colocci ²⁸, G. Conesa Balbastre ⁷⁰, Z. Conesa del Valle ⁵⁰, M.E. Connors ¹³⁵, J.G. Contreras ^{39,11}, T.M. Cormier ⁸³, Y. Corrales Morales ²⁷, I. Cortés Maldonado ², P. Cortese ³², M.R. Cosentino ¹¹⁸, F. Costa ³⁶, P. Crochet ⁶⁹, R. Cruz Albino ¹¹, E. Cuautle ⁶², L. Cunqueiro ³⁶, T. Dahms ⁹¹, A. Dainese ¹⁰⁷, A. Danu ⁶¹, D. Das ¹⁰⁰, I. Das ^{100,50}, S. Das ⁴, A. Dash ¹¹⁹, S. Dash ⁴⁷, S. De ^{130,118}, A. De Caro ^{31,12}, G. de Cataldo ¹⁰³, J. de Cuveland ⁴², A. De Falco ²⁵, D. De Gruttola ^{12,31}, N. De Marco ¹¹⁰, S. De Pasquale ³¹, A. Deisting ^{96,92}, A. Deloff ⁷⁶, E. Dénes ¹³⁴, G. D'Erasmo ³³, D. Di Bari ³³, A. Di Mauro ³⁶, P. Di Nezza ⁷¹, M.A. Diaz Corchero ¹⁰, T. Dietel ⁸⁸, P. Dillenseger ⁵², R. Divià ³⁶, Ø. Djupsland ¹⁸, A. Dobrin ^{56,80}, T. Dobrowolski ^{76,i}, D. Domenicis Gimenez ¹¹⁸, B. Dönigus ⁵², O. Dordic ²², A.K. Dubey ¹³⁰, A. Dubla ⁵⁶, L. Ducroux ¹²⁸, P. Dupieux ⁶⁹, R.J. Ehlers ¹³⁵, D. Elia ¹⁰³, H. Engel ⁵¹, B. Erazmus ^{112,36}, F. Erhardt ¹²⁷, D. Eschweiler ⁴², B. Espagnon ⁵⁰, M. Estienne ¹¹², S. Esumi ¹²⁶, D. Evans ¹⁰¹, S. Evdokimov ¹¹¹, G. Eyyubova ³⁹, L. Fabbietti ⁹¹, D. Fabris ¹⁰⁷, J. Faivre ⁷⁰, A. Fantoni ⁷¹, M. Fasel ⁷³, L. Feldkamp ⁵³, D. Felea ⁶¹, A. Feliciello ¹¹⁰, G. Feofilov ¹²⁹, J. Ferencei ⁸², A. Fernández Téllez ², E.G. Ferreiro ¹⁷, A. Ferretti ²⁷, A. Festanti ³⁰, J. Figiel ¹¹⁵, M.A.S. Figueiredo ¹²², S. Filchagin ⁹⁸, D. Finogeev ⁵⁵, F.M. Fionda ¹⁰³, E.M. Fiore ³³, M.G. Fleck ⁹², M. Floris ³⁶, S. Foertsch ⁶⁴, P. Foka ⁹⁶, S. Fokin ⁹⁹, E. Fragiocomo ¹⁰⁹, A. Francescon ^{36,30}, U. Frankenfeld ⁹⁶, U. Fuchs ³⁶, C. Furget ⁷⁰, A. Furs ⁵⁵, M. Fusco Girard ³¹, J.J. Gaardhøje ⁷⁹, M. Gagliardi ²⁷, A.M. Gago ¹⁰², M. Gallio ²⁷, D.R. Gangadharan ⁷³, P. Ganoti ⁸⁷, C. Gao ⁷, C. Garabatos ⁹⁶, E. Garcia-Solis ¹³, C. Gargiulo ³⁶, P. Gasik ⁹¹, M. Germain ¹¹², A. Gheata ³⁶, M. Gheata ^{61,36}, P. Ghosh ¹³⁰, S.K. Ghosh ⁴, P. Gianotti ⁷¹, P. Giubellino ^{36,110}, P. Giubilato ³⁰, E. Gladysz-Dziadus ¹¹⁵, P. Glässel ⁹², A. Gomez Ramirez ⁵¹, P. González-Zamora ¹⁰, S. Gorbunov ⁴², L. Görlich ¹¹⁵, S. Gotovac ¹¹⁴, V. Grabski ⁶³, L.K. Graczykowski ¹³², A. Grelli ⁵⁶, A. Grigoras ³⁶, C. Grigoras ³⁶, V. Grigoriev ⁷⁵, A. Grigoryan ¹, S. Grigoryan ⁶⁵, B. Grinyov ³, N. Grion ¹⁰⁹, J.F. Grosse-Oetringhaus ³⁶, J.-Y. Grossiord ¹²⁸, R. Grossi ³⁶, F. Guber ⁵⁵, R. Guernane ⁷⁰, B. Guerzoni ²⁸, K. Gulbrandsen ⁷⁹, H. Gulkanyan ¹, T. Gunji ¹²⁵, A. Gupta ⁸⁹, R. Gupta ⁸⁹, R. Haake ⁵³, Ø. Haaland ¹⁸, C. Hadjidakis ⁵⁰, M. Haiduc ⁶¹, H. Hamagaki ¹²⁵, G. Hamar ¹³⁴, L.D. Hanratty ¹⁰¹, A. Hansen ⁷⁹, J.W. Harris ¹³⁵, H. Hartmann ⁴², A. Harton ¹³, D. Hatzifotiadou ¹⁰⁴, S. Hayashi ¹²⁵, S.T. Heckel ⁵², M. Heide ⁵³, H. Helstrup ³⁷, A. Herghelegiu ⁷⁷, G. Herrera Corral ¹¹, B.A. Hess ³⁵, K.F. Hetland ³⁷, T.E. Hilden ⁴⁵, H. Hillemanns ³⁶, B. Hippolyte ⁵⁴, P. Hristov ³⁶, M. Huang ¹⁸, T.J. Humanic ²⁰, N. Hussain ⁴⁴, T. Hussain ¹⁹, D. Hutter ⁴², D.S. Hwang ²¹, R. Ilkaev ⁹⁸, I. Ilkiv ⁷⁶, M. Inaba ¹²⁶, C. Ionita ³⁶, M. Ippolitov ^{75,99}, M. Irfan ¹⁹, M. Ivanov ⁹⁶, V. Ivanov ⁸⁴, V. Izucheev ¹¹¹, A. Jacholkowski ²⁹, P.M. Jacobs ⁷³, C. Jahnke ¹¹⁸, H.J. Jang ⁶⁷, M.A. Janik ¹³², P.H.S.Y. Jayarathna ¹²⁰, C. Jena ³⁰, S. Jena ¹²⁰, R.T. Jimenez Bustamante ⁶², P.G. Jones ¹⁰¹, H. Jung ⁴³, A. Jusko ¹⁰¹, P. Kalinak ⁵⁸, A. Kalweit ³⁶, J. Kamin ⁵², J.H. Kang ¹³⁶, V. Kaplin ⁷⁵, S. Kar ¹³⁰, A. Karasu Uysal ⁶⁸, O. Karavichev ⁵⁵, T. Karavicheva ⁵⁵, E. Karpechev ⁵⁵, U. Kebschull ⁵¹, R. Keidel ¹³⁷, D.L.D. Keijdener ⁵⁶, M. Keil ³⁶, K.H. Khan ¹⁶, M.M. Khan ¹⁹, P. Khan ¹⁰⁰, S.A. Khan ¹³⁰, A. Khanzadeev ⁸⁴, Y. Kharlov ¹¹¹, B. Kileng ³⁷, B. Kim ¹³⁶, D.W. Kim ^{67,43}, D.J. Kim ¹²¹, H. Kim ¹³⁶, J.S. Kim ⁴³, M. Kim ⁴³,

- M. Kim ¹³⁶, S. Kim ²¹, T. Kim ¹³⁶, S. Kirsch ⁴², I. Kisel ⁴², S. Kiselev ⁵⁷, A. Kisiel ¹³², G. Kiss ¹³⁴, J.L. Klay ⁶, C. Klein ⁵², J. Klein ⁹², C. Klein-Bösing ⁵³, A. Kluge ³⁶, M.L. Knichel ⁹², A.G. Knospe ¹¹⁶, T. Kobayashi ¹²⁶, C. Kobdaj ¹¹³, M. Kofarago ³⁶, M.K. Köhler ⁹⁶, T. Kollegger ^{96,42}, A. Kolojvari ¹²⁹, V. Kondratiev ¹²⁹, N. Kondratyeva ⁷⁵, E. Kondratyuk ¹¹¹, A. Konevskikh ⁵⁵, C. Kouzinopoulos ³⁶, V. Kovalenko ¹²⁹, M. Kowalski ^{115,36}, S. Kox ⁷⁰, G. Koyithatta Meethaleveedu ⁴⁷, J. Kral ¹²¹, I. Králík ⁵⁸, A. Kravčáková ⁴⁰, M. Krelina ³⁹, M. Kretz ⁴², M. Krivda ^{58,101}, F. Krizek ⁸², E. Kryshen ³⁶, M. Krzewicki ^{42,96}, A.M. Kubera ²⁰, V. Kučera ⁸², Y. Kucheriaev ^{99,i}, T. Kugathasan ³⁶, C. Kuhn ⁵⁴, P.G. Kuijer ⁸⁰, I. Kulakov ⁴², J. Kumar ⁴⁷, L. Kumar ^{78,86}, P. Kurashvili ⁷⁶, A. Kurepin ⁵⁵, A.B. Kurepin ⁵⁵, A. Kuryakin ⁹⁸, S. Kushpil ⁸², M.J. Kweon ⁴⁹, Y. Kwon ¹³⁶, S.L. La Pointe ¹¹⁰, P. La Rocca ²⁹, C. Lagana Fernandes ¹¹⁸, I. Lakomov ^{50,36}, R. Langoy ⁴¹, C. Lara ⁵¹, A. Lardeux ¹⁵, A. Lattuca ²⁷, E. Laudi ³⁶, R. Lea ²⁶, L. Leardini ⁹², G.R. Lee ¹⁰¹, S. Lee ¹³⁶, I. Legrand ³⁶, J. Lehnhert ⁵², R.C. Lemmon ⁸¹, V. Lenti ¹⁰³, E. Leogrande ⁵⁶, I. León Monzón ¹¹⁷, M. Leoncino ²⁷, P. Lévai ¹³⁴, S. Li ^{7,69}, X. Li ¹⁴, J. Lien ⁴¹, R. Lietava ¹⁰¹, S. Lindal ²², V. Lindenstruth ⁴², C. Lippmann ⁹⁶, M.A. Lisa ²⁰, H.M. Ljunggren ³⁴, D.F. Lodato ⁵⁶, P.I. Loenne ¹⁸, V.R. Loggins ¹³³, V. Loginov ⁷⁵, C. Loizides ⁷³, X. Lopez ⁶⁹, E. López Torres ⁹, A. Lowe ¹³⁴, X.-G. Lu ⁹², P. Luettig ⁵², M. Lunardon ³⁰, G. Luparello ^{26,56}, A. Maevskaia ⁵⁵, M. Mager ³⁶, S. Mahajan ⁸⁹, S.M. Mahmood ²², A. Maire ⁵⁴, R.D. Majka ¹³⁵, M. Malaev ⁸⁴, I. Maldonado Cervantes ⁶², L. Malinina ⁶⁵, D. Mal'Kevich ⁵⁷, P. Malzacher ⁹⁶, A. Mamonov ⁹⁸, L. Manceau ¹¹⁰, V. Manko ⁹⁹, F. Manso ⁶⁹, V. Manzari ^{36,103}, M. Marchisone ²⁷, J. Mareš ⁵⁹, G.V. Margagliotti ²⁶, A. Margotti ¹⁰⁴, J. Margutti ⁵⁶, A. Marín ⁹⁶, C. Markert ¹¹⁶, M. Marquard ⁵², I. Martashvili ¹²³, N.A. Martin ⁹⁶, J. Martin Blanco ¹¹², P. Martinengo ³⁶, M.I. Martínez ², G. Martínez García ¹¹², M. Martinez Pedreira ³⁶, Y. Martynov ³, A. Mas ¹¹⁸, S. Masciocchi ⁹⁶, M. Masera ²⁷, A. Masoni ¹⁰⁵, L. Massacrier ¹¹², A. Mastroserio ³³, A. Matyja ¹¹⁵, C. Mayer ¹¹⁵, J. Mazer ¹²³, M.A. Mazzoni ¹⁰⁸, D. McDonald ¹²⁰, F. Meddi ²⁴, A. Menchaca-Rocha ⁶³, E. Meninno ³¹, J. Mercado Pérez ⁹², M. Meres ³⁸, Y. Miake ¹²⁶, M.M. Mieskolainen ⁴⁵, K. Mikhaylov ^{57,65}, L. Milano ³⁶, J. Milosevic ^{22,131}, L.M. Minervini ^{103,23}, A. Mischke ⁵⁶, A.N. Mishra ⁴⁸, D. Miśkowiec ⁹⁶, J. Mitra ¹³⁰, C.M. Mitu ⁶¹, N. Mohammadi ⁵⁶, B. Mohanty ^{130,78}, L. Molnar ⁵⁴, L. Montaño Zetina ¹¹, E. Montes ¹⁰, M. Morando ³⁰, S. Moretto ³⁰, A. Morreale ¹¹², A. Morsch ³⁶, V. Muccifora ⁷¹, E. Mudnic ¹¹⁴, D. Mühlheim ⁵³, S. Muhuri ¹³⁰, M. Mukherjee ¹³⁰, H. Müller ³⁶, J.D. Mulligan ¹³⁵, M.G. Munhoz ¹¹⁸, S. Murray ⁶⁴, L. Musa ³⁶, J. Musinsky ⁵⁸, B.K. Nandi ⁴⁷, R. Nania ¹⁰⁴, E. Nappi ¹⁰³, M.U. Naru ¹⁶, C. Nattrass ¹²³, K. Nayak ⁷⁸, T.K. Nayak ¹³⁰, S. Nazarenko ⁹⁸, A. Nedosekin ⁵⁷, L. Nellen ⁶², F. Ng ¹²⁰, M. Nicassio ⁹⁶, M. Niculescu ^{36,61}, J. Niedziela ³⁶, B.S. Nielsen ⁷⁹, S. Nikolaev ⁹⁹, S. Nikulin ⁹⁹, V. Nikulin ⁸⁴, F. Noferini ^{104,12}, P. Nomokonov ⁶⁵, G. Nooren ⁵⁶, J. Norman ¹²², A. Nyanin ⁹⁹, J. Nystrand ¹⁸, H. Oeschler ⁹², S. Oh ¹³⁵, S.K. Oh ⁶⁶, A. Ohlson ³⁶, A. Okatan ⁶⁸, T. Okubo ⁴⁶, L. Olah ¹³⁴, J. Oleniacz ¹³², A.C. Oliveira Da Silva ¹¹⁸, M.H. Oliver ¹³⁵, J. Onderwaater ⁹⁶, C. Oppedisano ¹¹⁰, A. Ortiz Velasquez ⁶², A. Oskarsson ³⁴, J. Otwinowski ^{96,115}, K. Oyama ⁹², M. Ozdemir ⁵², Y. Pachmayer ⁹², P. Pagano ³¹, G. Paić ⁶², C. Pajares ¹⁷, S.K. Pal ¹³⁰, J. Pan ¹³³, A.K. Pandey ⁴⁷, D. Pant ⁴⁷, V. Papikyan ¹, G.S. Pappalardo ¹⁰⁶, P. Pareek ⁴⁸, W.J. Park ⁹⁶, S. Parmar ⁸⁶, A. Passfeld ⁵³, V. Paticchio ¹⁰³, B. Paul ¹⁰⁰, T. Pawlak ¹³², T. Peitzmann ⁵⁶, H. Pereira Da Costa ¹⁵, E. Pereira De Oliveira Filho ¹¹⁸, D. Peresunko ^{75,99}, C.E. Pérez Lara ⁸⁰, V. Peskov ⁵², Y. Pestov ⁵, V. Petráček ³⁹, V. Petrov ¹¹¹, M. Petrovici ⁷⁷, C. Petta ²⁹, S. Piano ¹⁰⁹, M. Pikna ³⁸, P. Pillot ¹¹², O. Pinazza ^{104,36}, L. Pinsky ¹²⁰, D.B. Piyarathna ¹²⁰, M. Płoskoń ⁷³, M. Planinic ¹²⁷, J. Pluta ¹³², S. Pochybova ¹³⁴, P.L.M. Podesta-Lerma ¹¹⁷, M.G. Poghosyan ⁸⁵, B. Polichtchouk ¹¹¹, N. Poljak ¹²⁷, W. Poonsawat ¹¹³, A. Pop ⁷⁷, S. Porteboeuf-Houssais ⁶⁹, J. Porter ⁷³, J. Pospisil ⁸², S.K. Prasad ⁴, R. Preghenella ^{104,36}, F. Prino ¹¹⁰, C.A. Pruneau ¹³³, I. Pshenichnov ⁵⁵, M. Puccio ¹¹⁰, G. Puddu ²⁵, P. Pujahari ¹³³, V. Punin ⁹⁸, J. Putschke ¹³³, H. Qvigstad ²², A. Rachevski ¹⁰⁹, S. Raha ⁴, S. Rajput ⁸⁹, J. Rak ¹²¹, A. Rakotozafindrabe ¹⁵, L. Ramello ³², R. Raniwala ⁹⁰, S. Raniwala ⁹⁰, S.S. Räsänen ⁴⁵, B.T. Rascanu ⁵², D. Rathee ⁸⁶, V. Razazi ²⁵, K.F. Read ¹²³, J.S. Real ⁷⁰, K. Redlich ⁷⁶, R.J. Reed ¹³³, A. Rehman ¹⁸, P. Reichelt ⁵², M. Reicher ⁵⁶, F. Reidt ^{92,36}, X. Ren ⁷, R. Renfordt ⁵², A.R. Reolon ⁷¹, A. Reshetin ⁵⁵, F. Rettig ⁴², J.-P. Revol ¹², K. Reygers ⁹², V. Riabov ⁸⁴, R.A. Ricci ⁷², T. Richert ³⁴, M. Richter ²², P. Riedler ³⁶, W. Riegler ³⁶, F. Riggi ²⁹, C. Ristea ⁶¹, A. Rivetti ¹¹⁰, E. Rocco ⁵⁶, M. Rodríguez Cahuantzi ^{11,2}, A. Rodriguez Manso ⁸⁰, K. Røed ²², E. Rogochaya ⁶⁵, D. Rohr ⁴², D. Röhrich ¹⁸, R. Romita ¹²², F. Ronchetti ⁷¹, L. Ronflette ¹¹², P. Rosnet ⁶⁹, A. Rossi ³⁶, F. Roukoutakis ⁸⁷, A. Roy ⁴⁸, C. Roy ⁵⁴, P. Roy ¹⁰⁰, A.J. Rubio Montero ¹⁰, R. Rui ²⁶, R. Russo ²⁷, E. Ryabinkin ⁹⁹, Y. Ryabov ⁸⁴, A. Rybicki ¹¹⁵, S. Sadovsky ¹¹¹, K. Šafařík ³⁶, B. Sahlmuller ⁵², P. Sahoo ⁴⁸, R. Sahoo ⁴⁸, S. Sahoo ⁶⁰,

- P.K. Sahu ⁶⁰, J. Saini ¹³⁰, S. Sakai ⁷¹, M.A. Saleh ¹³³, C.A. Salgado ¹⁷, J. Salzwedel ²⁰, S. Sambyal ⁸⁹, V. Samsonov ⁸⁴, X. Sanchez Castro ⁵⁴, L. Šádor ⁵⁸, A. Sandoval ⁶³, M. Sano ¹²⁶, G. Santagati ²⁹, D. Sarkar ¹³⁰, E. Scapparone ¹⁰⁴, F. Scarlassara ³⁰, R.P. Scharenberg ⁹⁴, C. Schiaua ⁷⁷, R. Schicker ⁹², C. Schmidt ⁹⁶, H.R. Schmidt ³⁵, S. Schuchmann ⁵², J. Schukraft ³⁶, M. Schulc ³⁹, T. Schuster ¹³⁵, Y. Schutz ^{112,36}, K. Schwarz ⁹⁶, K. Schweda ⁹⁶, G. Scioli ²⁸, E. Scomparin ¹¹⁰, R. Scott ¹²³, K.S. Seeder ¹¹⁸, J.E. Seger ⁸⁵, Y. Sekiguchi ¹²⁵, I. Selyuzhenkov ⁹⁶, K. Senosi ⁶⁴, J. Seo ^{66,95}, E. Serradilla ^{10,63}, A. Sevcenco ⁶¹, A. Shabanov ⁵⁵, A. Shabetai ¹¹², O. Shadura ³, R. Shahoyan ³⁶, A. Shangaraev ¹¹¹, A. Sharma ⁸⁹, N. Sharma ^{60,123}, K. Shigaki ⁴⁶, K. Shtejer ^{9,27}, Y. Sibiriak ⁹⁹, S. Siddhanta ¹⁰⁵, K.M. Sielewicz ³⁶, T. Siemianczuk ⁷⁶, D. Silvermyr ^{83,34}, C. Silvestre ⁷⁰, G. Simatovic ¹²⁷, G. Simonetti ³⁶, R. Singaraju ¹³⁰, R. Singh ^{89,78}, S. Singha ^{78,130}, V. Singhal ¹³⁰, B.C. Sinha ¹³⁰, T. Sinha ¹⁰⁰, B. Sitar ³⁸, M. Sitta ³², T.B. Skaali ²², M. Slupecki ¹²¹, N. Smirnov ¹³⁵, R.J.M. Snellings ⁵⁶, T.W. Snellman ¹²¹, C. Søgaard ³⁴, R. Soltz ⁷⁴, J. Song ⁹⁵, M. Song ¹³⁶, Z. Song ⁷, F. Soramel ³⁰, S. Sorensen ¹²³, M. Spacek ³⁹, E. Spiriti ⁷¹, I. Sputowska ¹¹⁵, M. Spyropoulou-Stassinaki ⁸⁷, B.K. Srivastava ⁹⁴, J. Stachel ⁹², I. Stan ⁶¹, G. Stefanek ⁷⁶, M. Steinpreis ²⁰, E. Stenlund ³⁴, G. Steyn ⁶⁴, J.H. Stiller ⁹², D. Stocco ¹¹², P. Strmen ³⁸, A.A.P. Suaide ¹¹⁸, T. Sugitate ⁴⁶, C. Suire ⁵⁰, M. Suleymanov ¹⁶, R. Sultanov ⁵⁷, M. Šumbera ⁸², T.J.M. Symons ⁷³, A. Szabo ³⁸, A. Szanto de Toledo ^{118,i}, I. Szarka ³⁸, A. Szczepankiewicz ³⁶, M. Szymanski ¹³², J. Takahashi ¹¹⁹, N. Tanaka ¹²⁶, M.A. Tangaro ³³, J.D. Tapia Takaki ^{50,ii}, A. Tarantola Peloni ⁵², M. Tariq ¹⁹, M.G. Tarzila ⁷⁷, A. Tauro ³⁶, G. Tejeda Muñoz ², A. Telesca ³⁶, K. Terasaki ¹²⁵, C. Terrevoli ^{30,25}, B. Teyssier ¹²⁸, J. Thäder ^{96,73}, D. Thomas ^{56,116}, R. Tieulent ¹²⁸, A.R. Timmins ¹²⁰, A. Toia ⁵², S. Trogolo ¹¹⁰, V. Trubnikov ³, W.H. Trzaska ¹²¹, T. Tsuji ¹²⁵, A. Tumkin ⁹⁸, R. Turrisi ¹⁰⁷, T.S. Tveter ²², K. Ullaland ¹⁸, A. Uras ¹²⁸, G.L. Usai ²⁵, A. Utrobiticic ¹²⁷, M. Vajzer ⁸², M. Vala ⁵⁸, L. Valencia Palomo ⁶⁹, S. Vallero ²⁷, J. Van Der Maarel ⁵⁶, J.W. Van Hoorn ³⁶, M. van Leeuwen ⁵⁶, T. Vanat ⁸², P. Vande Vyvre ³⁶, D. Varga ¹³⁴, A. Vargas ², M. Vargyas ¹²¹, R. Varma ⁴⁷, M. Vasileiou ⁸⁷, A. Vasiliev ⁹⁹, A. Vauthier ⁷⁰, V. Vechernin ¹²⁹, A.M. Veen ⁵⁶, M. Veldhoen ⁵⁶, A. Velure ¹⁸, M. Venaruzzo ⁷², E. Vercellin ²⁷, S. Vergara Limón ², R. Vernet ⁸, M. Verweij ¹³³, L. Vickovic ¹¹⁴, G. Viesti ^{30,i}, J. Viinikainen ¹²¹, Z. Vilakazi ¹²⁴, O. Villalobos Baillie ¹⁰¹, A. Vinogradov ⁹⁹, L. Vinogradov ¹²⁹, Y. Vinogradov ⁹⁸, T. Virgili ³¹, V. Vislavicius ³⁴, Y.P. Viyogi ¹³⁰, A. Vodopyanov ⁶⁵, M.A. Völk ⁹², K. Voloshin ⁵⁷, S.A. Voloshin ¹³³, G. Volpe ^{36,134}, B. von Haller ³⁶, I. Vorobyev ⁹¹, D. Vranic ^{96,36}, J. Vrláková ⁴⁰, B. Vulpecu ⁶⁹, A. Vyushin ⁹⁸, B. Wagner ¹⁸, J. Wagner ⁹⁶, H. Wang ⁵⁶, M. Wang ^{7,112}, Y. Wang ⁹², D. Watanabe ¹²⁶, M. Weber ^{36,120}, S.G. Weber ⁹⁶, J.P. Wessels ⁵³, U. Westerhoff ⁵³, J. Wiechula ³⁵, J. Wikne ²², M. Wilde ⁵³, G. Wilk ⁷⁶, J. Wilkinson ⁹², M.C.S. Williams ¹⁰⁴, B. Windelband ⁹², M. Winn ⁹², C.G. Yaldo ¹³³, Y. Yamaguchi ¹²⁵, H. Yang ⁵⁶, P. Yang ⁷, S. Yano ⁴⁶, S. Yasnopolskiy ⁹⁹, Z. Yin ⁷, H. Yokoyama ¹²⁶, I.-K. Yoo ⁹⁵, V. Yurchenko ³, I. Yushmanov ⁹⁹, A. Zaborowska ¹³², V. Zaccole ⁷⁹, A. Zaman ¹⁶, C. Zampolli ¹⁰⁴, H.J.C. Zanolli ¹¹⁸, S. Zaporozhets ⁶⁵, A. Zarochentsev ¹²⁹, P. Závada ⁵⁹, N. Zaviyalov ⁹⁸, H. Zbroszczyk ¹³², I.S. Zgura ⁶¹, M. Zhalov ⁸⁴, H. Zhang ^{18,7}, X. Zhang ⁷³, Y. Zhang ⁷, C. Zhao ²², N. Zhigareva ⁵⁷, D. Zhou ⁷, Y. Zhou ⁵⁶, Z. Zhou ¹⁸, H. Zhu ^{7,18}, J. Zhu ^{7,112}, X. Zhu ⁷, A. Zichichi ^{12,28}, A. Zimmermann ⁹², M.B. Zimmermann ^{53,36}, G. Zinovjev ³, M. Zyzak ⁴²

¹ A.I. Alikhanyan National Science Laboratory (Yerevan Physics Institute) Foundation, Yerevan, Armenia² Benemerita Universidad Autónoma de Puebla, Puebla, Mexico³ Bogolyubov Institute for Theoretical Physics, Kiev, Ukraine⁴ Bose Institute, Department of Physics and Centre for Astroparticle Physics and Space Science (CAPSS), Kolkata, India⁵ Budker Institute for Nuclear Physics, Novosibirsk, Russia⁶ California Polytechnic State University, San Luis Obispo, CA, United States⁷ Central China Normal University, Wuhan, China⁸ Centre de Calcul de l'IN2P3, Villeurbanne, France⁹ Centro de Aplicaciones Tecnológicas y Desarrollo Nuclear (CEADEN), Havana, Cuba¹⁰ Centro de Investigaciones Energéticas Medioambientales y Tecnológicas (CIEMAT), Madrid, Spain¹¹ Centro de Investigación y de Estudios Avanzados (CINVESTAV), Mexico City and Mérida, Mexico¹² Centro Fermi – Museo Storico della Fisica e Centro Studi e Ricerche “Enrico Fermi”, Rome, Italy¹³ Chicago State University, Chicago, IL, United States¹⁴ China Institute of Atomic Energy, Beijing, China¹⁵ Commissariat à l’Energie Atomique, IRFU, Saclay, France¹⁶ COMSATS Institute of Information Technology (CIIT), Islamabad, Pakistan¹⁷ Departamento de Física de Partículas and IGFAE, Universidad de Santiago de Compostela, Santiago de Compostela, Spain¹⁸ Department of Physics and Technology, University of Bergen, Bergen, Norway¹⁹ Department of Physics, Aligarh Muslim University, Aligarh, India²⁰ Department of Physics, Ohio State University, Columbus, OH, United States²¹ Department of Physics, Sejong University, Seoul, South Korea²² Department of Physics, University of Oslo, Oslo, Norway

- ²³ Dipartimento di Elettrotecnica ed Elettronica del Politecnico, Bari, Italy
²⁴ Dipartimento di Fisica dell'Università 'La Sapienza' and Sezione INFN, Rome, Italy
²⁵ Dipartimento di Fisica dell'Università and Sezione INFN, Cagliari, Italy
²⁶ Dipartimento di Fisica dell'Università and Sezione INFN, Trieste, Italy
²⁷ Dipartimento di Fisica dell'Università and Sezione INFN, Turin, Italy
²⁸ Dipartimento di Fisica e Astronomia dell'Università and Sezione INFN, Bologna, Italy
²⁹ Dipartimento di Fisica e Astronomia dell'Università and Sezione INFN, Catania, Italy
³⁰ Dipartimento di Fisica e Astronomia dell'Università and Sezione INFN, Padova, Italy
³¹ Dipartimento di Fisica 'E.R. Caianiello' dell'Università and Gruppo Collegato INFN, Salerno, Italy
³² Dipartimento di Scienze e Innovazione Tecnologica dell'Università del Piemonte Orientale and Gruppo Collegato INFN, Alessandria, Italy
³³ Dipartimento Interateneo di Fisica 'M. Merlin' and Sezione INFN, Bari, Italy
³⁴ Division of Experimental High Energy Physics, University of Lund, Lund, Sweden
³⁵ Eberhard Karls Universität Tübingen, Tübingen, Germany
³⁶ European Organization for Nuclear Research (CERN), Geneva, Switzerland
³⁷ Faculty of Engineering, Bergen University College, Bergen, Norway
³⁸ Faculty of Mathematics, Physics and Informatics, Comenius University, Bratislava, Slovakia
³⁹ Faculty of Nuclear Sciences and Physical Engineering, Czech Technical University in Prague, Prague, Czech Republic
⁴⁰ Faculty of Science, P.J. Šafárik University, Košice, Slovakia
⁴¹ Faculty of Technology, Buskerud and Vestfold University College, Vestfold, Norway
⁴² Frankfurt Institute for Advanced Studies, Johann Wolfgang Goethe-Universität Frankfurt, Frankfurt, Germany
⁴³ Gangneung-Wonju National University, Gangneung, South Korea
⁴⁴ Gauhati University, Department of Physics, Gauhati, India
⁴⁵ Helsinki Institute of Physics (HIP), Helsinki, Finland
⁴⁶ Hiroshima University, Hiroshima, Japan
⁴⁷ Indian Institute of Technology Bombay (IIT), Mumbai, India
⁴⁸ Indian Institute of Technology Indore, Indore (IITI), India
⁴⁹ Inha University, Incheon, South Korea
⁵⁰ Institut de Physique Nucléaire d'Orsay (IPNO), Université Paris-Sud, CNRS-IN2P3, Orsay, France
⁵¹ Institut für Informatik, Johann Wolfgang Goethe-Universität Frankfurt, Frankfurt, Germany
⁵² Institut für Kernphysik, Johann Wolfgang Goethe-Universität Frankfurt, Frankfurt, Germany
⁵³ Institut für Kernphysik, Westfälische Wilhelms-Universität Münster, Münster, Germany
⁵⁴ Institut Pluridisciplinaire Hubert Curien (IPHC), Université de Strasbourg, CNRS-IN2P3, Strasbourg, France
⁵⁵ Institute for Nuclear Research, Academy of Sciences, Moscow, Russia
⁵⁶ Institute for Subatomic Physics of Utrecht University, Utrecht, Netherlands
⁵⁷ Institute for Theoretical and Experimental Physics, Moscow, Russia
⁵⁸ Institute of Experimental Physics, Slovak Academy of Sciences, Košice, Slovakia
⁵⁹ Institute of Physics, Academy of Sciences of the Czech Republic, Prague, Czech Republic
⁶⁰ Institute of Physics, Bhubaneswar, India
⁶¹ Institute of Space Science (ISS), Bucharest, Romania
⁶² Instituto de Ciencias Nucleares, Universidad Nacional Autónoma de México, Mexico City, Mexico
⁶³ Instituto de Física, Universidad Nacional Autónoma de México, Mexico City, Mexico
⁶⁴ iThemba LABS, National Research Foundation, Somerset West, South Africa
⁶⁵ Joint Institute for Nuclear Research (JINR), Dubna, Russia
⁶⁶ Konkuk University, Seoul, South Korea
⁶⁷ Korea Institute of Science and Technology Information, Daejeon, South Korea
⁶⁸ KTO Karatay University, Konya, Turkey
⁶⁹ Laboratoire de Physique Corpusculaire (LPC), Clermont Université, Université Blaise Pascal, CNRS-IN2P3, Clermont-Ferrand, France
⁷⁰ Laboratoire de Physique Subatomique et de Cosmologie, Université Grenoble-Alpes, CNRS-IN2P3, Grenoble, France
⁷¹ Laboratori Nazionali di Frascati, INFN, Frascati, Italy
⁷² Laboratori Nazionali di Legnaro, INFN, Legnaro, Italy
⁷³ Lawrence Berkeley National Laboratory, Berkeley, CA, United States
⁷⁴ Lawrence Livermore National Laboratory, Livermore, CA, United States
⁷⁵ Moscow Engineering Physics Institute, Moscow, Russia
⁷⁶ National Centre for Nuclear Studies, Warsaw, Poland
⁷⁷ National Institute for Physics and Nuclear Engineering, Bucharest, Romania
⁷⁸ National Institute of Science Education and Research, Bhubaneswar, India
⁷⁹ Niels Bohr Institute, University of Copenhagen, Copenhagen, Denmark
⁸⁰ Nikhef, National Institute for Subatomic Physics, Amsterdam, Netherlands
⁸¹ Nuclear Physics Group, STFC Daresbury Laboratory, Daresbury, United Kingdom
⁸² Nuclear Physics Institute, Academy of Sciences of the Czech Republic, Řež u Prahy, Czech Republic
⁸³ Oak Ridge National Laboratory, Oak Ridge, TN, United States
⁸⁴ Petersburg Nuclear Physics Institute, Gatchina, Russia
⁸⁵ Physics Department, Creighton University, Omaha, NE, United States
⁸⁶ Physics Department, Panjab University, Chandigarh, India
⁸⁷ Physics Department, University of Athens, Athens, Greece
⁸⁸ Physics Department, University of Cape Town, Cape Town, South Africa
⁸⁹ Physics Department, University of Jammu, Jammu, India
⁹⁰ Physics Department, University of Rajasthan, Jaipur, India
⁹¹ Physik Department, Technische Universität München, Munich, Germany
⁹² Physikalisches Institut, Ruprecht-Karls-Universität Heidelberg, Heidelberg, Germany
⁹³ Politecnico di Torino, Turin, Italy
⁹⁴ Purdue University, West Lafayette, IN, United States
⁹⁵ Pusan National University, Pusan, South Korea
⁹⁶ Research Division and ExtreMe Matter Institute EMMI, GSI Helmholtzzentrum für Schwerionenforschung, Darmstadt, Germany
⁹⁷ Rudjer Bošković Institute, Zagreb, Croatia
⁹⁸ Russian Federal Nuclear Center (VNIIEF), Sarov, Russia
⁹⁹ Russian Research Centre Kurchatov Institute, Moscow, Russia
¹⁰⁰ Saha Institute of Nuclear Physics, Kolkata, India
¹⁰¹ School of Physics and Astronomy, University of Birmingham, Birmingham, United Kingdom

- ¹⁰² Sección Física, Departamento de Ciencias, Pontificia Universidad Católica del Perú, Lima, Peru
¹⁰³ Sezione INFN, Bari, Italy
¹⁰⁴ Sezione INFN, Bologna, Italy
¹⁰⁵ Sezione INFN, Cagliari, Italy
¹⁰⁶ Sezione INFN, Catania, Italy
¹⁰⁷ Sezione INFN, Padova, Italy
¹⁰⁸ Sezione INFN, Rome, Italy
¹⁰⁹ Sezione INFN, Trieste, Italy
¹¹⁰ Sezione INFN, Turin, Italy
¹¹¹ SSC IHEP of NRC Kurchatov institute, Protvino, Russia
¹¹² SUBATECH, Ecole des Mines de Nantes, Université de Nantes, CNRS-IN2P3, Nantes, France
¹¹³ Suranaree University of Technology, Nakhon Ratchasima, Thailand
¹¹⁴ Technical University of Split FESB, Split, Croatia
¹¹⁵ The Henryk Niewodniczanski Institute of Nuclear Physics, Polish Academy of Sciences, Cracow, Poland
¹¹⁶ The University of Texas at Austin, Physics Department, Austin, TX, United States
¹¹⁷ Universidad Autónoma de Sinaloa, Culiacán, Mexico
¹¹⁸ Universidade de São Paulo (USP), São Paulo, Brazil
¹¹⁹ Universidade Estadual de Campinas (UNICAMP), Campinas, Brazil
¹²⁰ University of Houston, Houston, TX, United States
¹²¹ University of Jyväskylä, Jyväskylä, Finland
¹²² University of Liverpool, Liverpool, United Kingdom
¹²³ University of Tennessee, Knoxville, TN, United States
¹²⁴ University of the Witwatersrand, Johannesburg, South Africa
¹²⁵ University of Tokyo, Tokyo, Japan
¹²⁶ University of Tsukuba, Tsukuba, Japan
¹²⁷ University of Zagreb, Zagreb, Croatia
¹²⁸ Université de Lyon, Université Lyon 1, CNRS/IN2P3, IPN-Lyon, Villeurbanne, France
¹²⁹ V. Fock Institute for Physics, St. Petersburg State University, St. Petersburg, Russia
¹³⁰ Variable Energy Cyclotron Centre, Kolkata, India
¹³¹ Vinča Institute of Nuclear Sciences, Belgrade, Serbia
¹³² Warsaw University of Technology, Warsaw, Poland
¹³³ Wayne State University, Detroit, MI, United States
¹³⁴ Wigner Research Centre for Physics, Hungarian Academy of Sciences, Budapest, Hungary
¹³⁵ Yale University, New Haven, CT, United States
¹³⁶ Yonsei University, Seoul, South Korea
¹³⁷ Zentrum für Technologietransfer und Telekommunikation (ZTT), Fachhochschule Worms, Worms, Germany

ⁱ Deceased.ⁱⁱ Also at: University of Kansas, Lawrence, Kansas, United States.